Hydrodynamics of wind-assisted ship propulsion validation of RANS-CFD methodology

van der Kolk, Nico; Keuning, Lex; Huijsmans, Rene

Publication date
2017

Document Version
Final published version

Published in
Proceedings of the 4th International Conference on Innovation in High Performance Sailing Yachts (INNOVSAIL 2017)

Citation (APA)
van der Kolk, N., Keuning, L., & Huijsmans, R. (2017). Hydrodynamics of wind-assisted ship propulsion validation of RANS-CFD methodology. In P. Bot (Ed.), *Proceedings of the 4th International Conference on Innovation in High Performance Sailing Yachts (INNOVSAIL 2017)* (pp. 207-216). Article 796 Sailing Yard Research Foundation (SYRF).

Important note
To cite this publication, please use the final published version (if applicable).
Please check the document version above.

HYDRODYNAMICS OF WIND-ASSISTED SHIP PROPULSION VALIDATION OF RANS-CFD METHODOLOGY

N.J. van der Kolk, Delft University of Technology, The Netherlands, n.j.vanderkolk@tudelft.nl
J.A. Keuning and **R.H.M. Huijsmans,** Delft University of Technology, The Netherlands, j.a.keuning@tudelft.nl, r.h.m.huijsmans@tudelft.nl

A Reynolds-Averaged Navier Stokes computational fluid dynamics (RANS-CFD) package will be one of the primary tools used during the development of a performance prediction program for Wind-Assisted commercial ships. The modelling challenge presented by large separated flow structures in the wake of the sailing ship points to a conscientious validation study. A validation data set, consisting of hydrodynamic forces acting on the ship sailing with a leeway angle, was collected at the Delft University of Technology towing tank facility, for bare-hull and appended cases. Four hull geometries were selected to represent of the Delft Wind-Assist Systematic Series. Appended cases were designed to represent a broad range of appendage topologies: Rudder, Bilge-keels, Skeg, and Barkeel. The direct validation exercise for the bare-hull case was successful, with the validation level for the sideforce equal to 9.5% (fine mesh: 9M cells). An extended validation statement is made for simulations for the entire series. This exercise was successful for leeway angles equal to $\beta = [3^o, 6^o]$. The validation level (base mesh, 3M cells) for each force component is:$u_{X\prime}$=12%, $u_{Y\prime}$=17%, $u_{N\prime}$=10%. The validation for appended geometries was not regarded as successful, with the exception of the Rudder case. The numerical uncertainty is the dominant contribution for the validation level, motivating a proportionate refinement of the grid. Here, it is sufficient to achieve parity with other contributions to the uncertainty within the larger context of the project.

NOMENCLATURE

β	Leeway angle (deg)
Θ	Placeholder for bias error contribution
μ_{Ens}	Mean value for $\mathrm{E_{Ens}}$ (%)
ρ	Density of water (kg.m^{-3})
σ_{Ens}	Standard deviation for $\mathrm{E_{Ens}}$ (%)
$\mathrm{B_\Theta}$	Bias error for Θ
C_{M}	Midship coefficient
C_{P}	Prismatic coefficient
C_{TS}	Coefficient for strip correction
$\mathrm{CI95_{Ens}}$	95% Confidence interval for $\mathrm{E_{Ens}}$ (%)
E	Comparison error (N)
$\mathrm{E_{\%}}$	Relative comparison error (%)
$\mathrm{E_{Ens}}$	Ensemble comparison error (%)
F_{X}	Resistance (N)
F_{Y}	Sideforce (N)
Fn	Froude number
L	Length (m)
N	Yaw moment (N.m)
P	Precision error (N)
T	Draft (m)
U	Expanded uncertainty (%)
u_{Val}	Validation standard uncertainty (%)
V	Vessel speed (m/s)
X'_Δ	Non-dimensionalisation for F_X by displacement
X'	Non-dimensionalisation for F_X
X'_{i}	Induced resistance
Y'	Non-dimensionalisation for F_Y
N'	Non-dimensionalisation for M_Z

1 INTRODUCTION

Wind as a source of energy for commercial ships has again garnered interest as an environmentally friendly propulsion alternative, as a possible response to volatile fuel prices, and to comply with increasingly exacting environmental regulations. The further development of this promising technology is hampered by a poor understanding of the interaction effects between wind propulsors and the hydromechanics of commercial ships. The Wind-Assisted Ship Propulsion (WASP) Performance Prediction Program, under development at the TU Delft, will provide designers the ability to explore the possibilities offered by wind as an auxiliary propulsor. For example, the well-known phenomenon of induced drag for lifting surfaces has a direct analogue for commercial ship types in the generation of hydrodynamic sideforce. Though the flow mechanisms only vaguely resemble the Prandtl wing and the associated derivation for the induced drag, the accounting for energy loss in shed vorticity is especially relevant for the present application. Following theories for low-aspect planforms [1], the induced drag may be significant for commercial ships, meaning that the thrust delivered by a wind propulsor might well be overwhelmed by this increase in resistance, negating the benefit of adding the wind propulsor. The tool is developed and documented in a rigorous and transparent way, so that the designer can confidently report performance figures for subsequent environmental and economic analyses.

With the WASP Performance Prediction Program, a designer is able to perform parametric investigations for

the arrangement of wind propulsors and the hull form geometry, and can eventually optimize a commercial hull form for sailing. Models that capture the behaviour of a generic commercial vessel under sail will be derived by studying the sensitivity of vessel performance to changes in hull geometry. For example, to determine the influence of vessel draft, vessel behaviour for increased and decreased draft is fit to some functional form. Of course, as other hull-form parameters are allowed to vary, the structure of this function will become increasingly complex. The force models for a generic hull would be determined by polynomial regression techniques from a large set of systematically varied hulls. In the past, this database for regression analysis was built using results from towing tank experiments. [2] The maturity of Reynolds-averaged Navier Stokes computational fluid dynamics (RANS-CFD) solvers offers the ready, inexpensive analysis for a large number of hull variations. However, simulations that remain computationally affordable may be unable to model the flow patterns occurring near a sailing commercial ship. A wind-assisted ship will operate with a leeway angle in order to generate the hydrodynamic sideforce needed for a sailing equilibrium. Fluid flow around the ship will experience separation effects and will become entrained in large vortices in the wake of the ship. Modelling the occurrence of separation and the evolution of these vortices is the principal simulation challenge, as both phenomena may challenge modelling assumptions made in the simulation setup.

In this paper, a validation exercise is described for the computationally affordable assessment of high volumes of ship-hull variations. Results are presented for bare-hull and appended-hull RANS-CFD simulations.

2 VALIDATION DATA SET

The validation dataset is composed of hulls from the Delft Wind-Assist Series. Each hull is tested at three speeds: Fn= 0.13, 0.17, 0.21, and four leeway angles: β= 0, 3, 6, 9. The validation data consists of global forces acting on the ship, expressed in the flow-aligned coordinate system. The forces are non-dimensionalised according to the manoeuvring convention.

$$X' = \frac{F_X}{\frac{1}{2}\rho V^2 TL} \quad (1)$$

$$Y' = \frac{F_Y}{\frac{1}{2}\rho V^2 TL} \quad (2)$$

$$N' = \frac{M_Z}{\frac{1}{2}\rho V^2 TL^2} \quad (3)$$

2.1 DELFT WIND-ASSIST SERIES

The hulls in the wind-assist series are systematic variations of Eco-liner hull, designed by Dykstra Naval Architects. The series comprises 42 hulls, for which the prismatic coefficient, the midship coefficient, the draft-to-length ratio, and the deadrise angle are systematically varied.

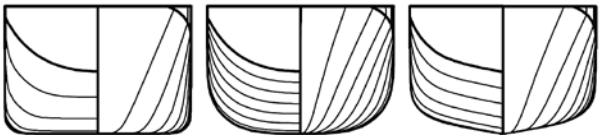

Figure 1 Bare hull validation cases (from left to right): Hull 16 – Bare (C_P^+ C_M^+), Hull 19 – Bare (C_P^- C_M^-), and Hull 34 – Bare (10^o $deadrise$). The lines plan for Hull 1 is not publicly available.

The variation for prismatic coefficient is effected by lengthening or shortening the parallel mid-body. The midship coefficient is modified by increasing and decreasing the bilge radius. For variations in the draft to length ratio, the displacement is kept constant by reducing the beam accordingly. Finally, the deadrise hulls are defined by extending a tangent line from the bilge to the centreline at the appropriate angle.

Table 1 Summary of Delft Wind-Assist Series

Hull	C_P	C_M	T/L	Deadrise
1 ($parent$)	0.764	0.942	0.047	0^0
16 (C_P^+ C_M^+)	0.840	0.984	0.047	0^0
19 (C_P^- C_M^-)	0.689	0.874	0.047	0^0
34 (10^o $deadrise$)	0.764	0.838	0.047	10^0
Min	0.686	0.787	0.042	0^0
Max	0.840	0.984	0.060	14^0

The extents of the systematic series and the geometry for validation cases are presented in Table 1. The validation cases were selected as representative hulls for the broader Wind-Assist series, and specifically to challenge the capabilities of the RANS-CFD modelling. Hull 1 and Hull 34 were selected as representative hulls for the series; Hull 1, being the parent hull at the center of all variations, and Hull 34 as the median case for the deadrise hulls. Hull 16, with sharp bilges, is expected to generate pronounced bilge vortices, challenging the capabilities of the fluid modelling in this respect. Hull 19, with a slender form and rounded bilges, will challenge the modelling for flow separation.

2.2 APPENDED GEOMETRIES

Hull 1 and Hull 34 were fitted with a series of appendages that was designed to represent a broad range of appendage topologies. Hull 1 was fitted with a Rudder and Bilge Keels. The rudder was mounted on a high precision quadrant that could be set to 0° and +/-6°. Hull 34 was fitted with a Skeg and a combination Skeg and Barkeel.

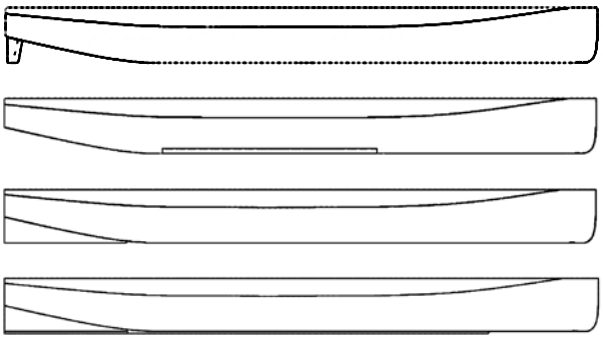

Figure 2 Overview of appended validation cases (from top to bottom): Hull 1 - Rudder, Hull 1 - Bilge Keels, Hull 34 - Skeg, Hull 34 - Skeg + Barkeel.

2.3 EXPERIMENTAL CAMPAIGNS

The validation data used in this exercise was collected during two experimental campaigns, in 2015 and in 2016. Hull 1 – Bare, Hull 16 – Bare, and Hull 19 – Bare were tested during the 2015 campaign [3]. Hull 34 – Bare and all appended cases were tested in 2016. With the intent to eventually make statements about the validation level of simulations, it is necessary to address any inconsistencies in the validation data set, especially as may pertain to the experimental uncertainty. Two items need to be addressed: the treatment for sinkage and trim, and the adoption of a uniform strip resistance coefficient. During the 2015 experiments, the model was mounted using the setup normally used for sailing yachts at Delft University of Technology [2]: free to trim and sink according to the speed and leeway angle. A fully restrained setup was used during the 2016 experiment, and all simulations were performed with heave and pitch constrained. In view of the low Froude numbers considered, a large discrepancy is not expected. The motivation for this change will be discussed further in Section 4. Finally, a uniform strip resistance coefficient was adopted, determined in 2016 for Hull 34. The post-processing for the 2015 experiment was revisited with the 2016 C_{TS} value.

3 VALIDATION METHODOLOGY

3.1 VALIDATION STATEMENT

The methodology for validation is adopted from the ITTC guideline [4] and from the American Society of Mechanical Engineers (ASME) standard [5]. A validation statement is made according to the relationship between the comparison error, defined as the difference between simulation and experimental values: $E = Sim - Exp$, and the validation standard uncertainty, u_{Val}, which is a combination of the uncertainties associated with the simulation and experimental data.

The following statements are possible:

$E < u_{\mathrm{Val}}$: The comparison error falls within uncertainty band defined by validation standard uncertainty. The simulation is validated with a the validation level equal to u_{Val}.

$E > u_{\mathrm{Val}}$: The comparison error is larger than the validation standard uncertainty, and the validation exercise fails.

Determining u_{Val} is thus a central task in the validation exercise. Following the derivation from the ASME standard, the error for a simulation result is separated into a component the rising due to the modelling assumptions and approximations (δ_{Model}), and a component arising from the numerical solution of the equations, (δ_{Num}). The numerical error is expressed as an uncertainty, u_{Num} [6] [7]. Assuming U_{Num} and U_{Exp} are uncorrelated, the following definition is adopted:

$$u_{\mathrm{Val}} = \sqrt{{U_{\mathrm{Num}}}^2 + {U_{\mathrm{Exp}}}^2} \tag{4}$$

3.2 MODELLING ERROR

Fluid flow around the sailing ship will experience separation effects and will become entrained in large vortices in the wake of the ship. As discussed in the introduction, the modelling of these phenomena is the principal simulation challenge. For this validation exercise, the extent to which these phenomena are captured is measured with the integration of pressure and shear stress over the hull, corresponding to the forces measured in experimental campaigns. Therefore, the flow field is only validated in so far as is manifest as forces on the hull. The validation procedure is carried out without modification for the case for $Fn = 0.17$ and $\beta = 9^0$, for which an estimate for the validation standard uncertainty is directly available. These results are presented in Section 7.

One objective of this validation exercise is to bound the modelling errors with a bandwidth defined by the validation standard uncertainty:

$$\delta_{\mathrm{Model}} \in [E - u_{\mathrm{Val}}\,, E + u_{\mathrm{Val}}] \tag{5}$$

An example of a model error, and a central complication for the validation data, is the possible effect of the turbulence stimulators on separation location and on the strength of any separated vortices (as determinants for the sideforce and yaw moments). In this case, one might argue that the simulation better resembles a real ship. However, the validation exercise measures the degree to which the simulation is able to reproduce experiments and the fault is therefore a modelling error for the simulation. Similarly, vessel sinkage and trim, which was allowed during the 2015 experiments and constrained for

the 2016 experiments, is constrained for all simulations. Although the 2016 experiment is less realistic one component of the simulation modelling error has been removed. The focus here is the test the capabilities of RANS-CFD for separated flow structures, and the validation cases might better be thought of as ship-like forms. An unambiguous categorization of numerical and the modelling errors is necessary to isolate and quantify the modelling error [5].

3.3 EXTENDED VALIDATION STATEMENT

A validation statement is made for the Delft Wind-Assist Series by assuming that the statistics for the comparison error of the validation cases will be representative of the entire wind assist series. For this analysis, the definition of the relative comparison error introduces some ambiguity when presenting an ensemble of results for several operating conditions. A relative comparison error might be defined as follows:

$$E_{\%} = (100) * \frac{Sim - Exp}{Exp} \tag{6}$$

Is this definition, a fault due to precision errors, which do not scale with the measurand, will be overstated for lower values and understated for larger values. For the sideforce in particular, the measured values vary over one order-of-magnitude. Instead, the comparison error is made relative using one half of the range of the measurands:

$$E_{\mathrm{Ens}} = (100) * \frac{Sim - Exp}{\frac{1}{2}\left(max(Exp) - min(Exp)\right)} \tag{7}$$

The validation standard uncertainty from the direct validation is adopted here without modification. The numerical uncertainty is only available for one hull and one operating condition, while the experimental uncertainty can be calculated for all conditions. It may be possible to assume an added numerical uncertainty, dependant on speed, leeway angle, or hull geometry, as the numerical uncertainty may plausibly scale with both speed and leeway angle, as an increase in the strength of shed vorticity should be commiserate with the uncertainty associated with the evaluation of flow gradients. Likewise, the hull geometry may influence simulation uncertainty; for example, the hull-surface curvature as a determinant for separation behaviour. The numerical uncertainty is the dominant contribution for the validation standard uncertainty. Therefore, rather than introduce a somewhat arbitrary added uncertainty, that would significantly relax the requirement for validation, the known estimate for the numerical uncertainty is kept unmodified. For the experimental uncertainty, the uncertainty for each case was approximately equal. As a conservative estimate, the largest uncertainty for each force component was adopted.

Following the same method as described above, the 95% confidence interval of the ensemble comparison error is compared to the extended validation uncertainty. The confidence interval is understood as an *estimate* for the range of the comparison errors. Finally, the evaluation of the hulls from the Delft Wind-Assist series using the RANS-CFD methodology presented herein is validated if the confidence interval for the ensemble comparison error of the validation cases is less than the extended validation standard uncertainty.

4 EXPERIMENTAL METHOD

4.1 EXPERIMENTAL SETUP

Experiments were designed to obtain validation data with minimal uncertainty. As detailed in Section 2, the validation data was collected during two experimental campaigns, in 2015 and 2016. The setup for the experiment was altered for the 2016 campaign. The fully constrained setup, with the six component measurement frame, rather than the sailing yacht set-up, gave better control over the position of the model, and provides extra flexibility when designing the arrangement of sensors; again with the aim to minimize experimental uncertainty. The uncertainty analysis for the 2015 testing campaign is summarized in Section 4. The 2016 experiments are described in the remainder of this section.

During the 2016 test campaign, the models were tested in fully captive setup. Mounting the ship beneath the hexapod oscillator gave precise control over the orientation of the model. The models were connected to the hexapod with the six component measurement frame. The measurement frame is designed to resolve any applied force or moment into orthogonal forces and moments. The arrangement of the sensors on the measurement frame was made to obtain the best possible fidelity for the transverse force components. The position of the model is recorded using a Certus optical tracking system. All signals are filtered with a low-pass filter set to 100 Hz before sampling to prevent aliasing. The signal is sampled at a frequency of 1000 Hz and written to disc.

The measurement campaign was three weeks long. To assure that a consistent procedure was followed, the following protocol was adopted:

1) Model set to zero leeway position for nul measurement.
2) Model set to leeway angle for second nul measurement.
3) Carriage accelerated to test speed. 10 seconds is allowed for the flow to reach a steady condition.
4) Measurements recorded for 60 seconds.

The nominal rest period between runs was 20 minutes. The test program is arranged so that high-speed runs were interspersed regularly, and so that a low-speed run

did not immediately follow a high-speed run. The first run of each day, and the first run after a weekend, was marked in the measurement log.

4.1.1 Turbulence Stimulators

The models were fitted with turbulence stimulators to ensure a turbulent boundary layer along the hull. The correction for an added resistance due to the strips was determined according to the standard ITTC practice [8]. The strip resistance coefficient was determined for Hull 34 - Bare. This value is adopted for all other data, including results from earlier tests.

4.1.2 Bow Wave Measurements

As a further validation for the simulations, the interface capturing for the asymmetric bow wave was compared to measurements from experiments. The profile of the bow wave was measured using cameras and grid markings on the ship. The images were de-warped to correct for lens effect and perspective and scaled so that one is pixel was equal to 0.5 mm. It was then possible to measure the position of the maximum and minimum wave elevation. This exercise was performed for Hull 34 - Bare.

4.2 EXPERIMENTAL UNCERTAINTY

The experimental uncertainty is determined according to the ITTC guideline for planar motion tests [9]. The following error components are considered to be significant: bias errors arising from the measurement of forces and moments with the six-component frame, bias errors arising from model misalignment in the tank, bias errors due to geometric faults in the model construction, and an end-to-end estimate of the precision error for the complete experimental setup. The calculation of $U_{X'}$ is detailed for Hull 34 - Bare at $Fn = 0.17$ and $\beta = 9^0$. This is the same operating condition used during the uncertainty estimation for the 2015 experiments.

4.2.1 Bias Errors

It is necessary to determine the sensitivity for each force component to each bias error. These expressions are given for X', defined as the partial derivative with respect to the quantity of interest:

$$\frac{\partial}{\partial F_X} X' = \frac{2}{\rho U^2 T L} \tag{8}$$

$$\frac{\partial}{\partial \beta} X' = X'_{beta} \tag{9}$$

$$\frac{\partial}{\partial T} X' = \frac{-2F_X}{\rho U^2 T^2 L} \tag{10}$$

The bias error for forces measured with the six-component frame was estimated by repeating the calibration process for the fully assembled frame. A variety of forces and moments were applied to the frame, and the disparity, including a significant hysteresis effect, was used as B_{F_X}. The hysteresis phenomena observed for strain gauges is exacerbated for the mechanically complex measurement frame. Anticipating that the vibrations of a moving carriage would encourage a settling of the frame, a set of measurement was made with a typical carriage speed. In fact the hysteresis effect was significantly reduced. The estimate for B_{F_X} is therefore likely a conservative value.

The alignment of the model for each case was measured with ten repeat runs, with five positive leeway angles and five negative leeway angles. This allowed for a test for the symmetry of the system and also gave an indication for the precision of the setup. These runs were arranged so that the position of the model was changed before each run, i.e., the model was not simply towed repeatedly for a single operating condition. For Hull 1 - Rudder, the rudder angle was set to positive and negative angles (five runs with +6° leeway, +6° rudder, and five runs with -6° leeway, -6° rudder). These runs were interspersed throughout the measurement campaign so that the ship position and rudder angle were altered before each repeat run. The bias error for leeway angle, B_β, was estimated using the X-intercept of the linear fit for these results. As a conservative estimate, a sum was made of the absolute offset determined using the sideforce and the yaw moment. This estimate for the bias might also contain the influence of an asymmetry in the model geometry. Finally, the bias error due to faults in the model geometry is assumed $B_T = 1.5$ mm.

The bias error for X' is expressed as an expanded uncertainty with 95% confidence level [10]:

$$B_{X'} = 2\sqrt{\left(\frac{\partial X'}{\partial F_X}\right)^2 B_{F_X}^2 + \left(\frac{\partial X'}{\partial \beta}\right)^2 B_\beta^2 + \left(\frac{\partial X'}{\partial T}\right) B_T^2} \tag{11}$$

4.2.2 Precision Errors

The repeatability of the measurement is an “end-to-end” test for the precision of the setup. The repeat runs are meant to capture any variations in the test condition over the duration of the test program.

Table 2 Details for calculation of experimental uncertainty for Hull 34 – Bare for $\boldsymbol{X'}$. The uncertainty $\boldsymbol{u'}$ is given as a percentage of the measured value. The precision error is the dominant term.

Θ	$\frac{\partial F_X}{\partial \Theta}$	δ_Θ	u_Θ [N]	u'_Θ [%]
F_X	0.014	0.0243 N	0.047	1.8%
β	0.012	0.17^0	0.010	0.4%
T	0.29	0.0015 m	0.059	2.3%
P	-	-	0.098	3.8%

Ten repeat runs (positive leeway angle only) were carried out for Hull 34 - Skeg, and this result for the precision of the setup was carried through for all hulls:

$$P_{X'} = 2.228 * \sigma_{X'} \quad (12)$$

The uncertainties are combined as uncorrelated quantities:

$$U_{X'} = \sqrt{{B_{X'}}^2 + {P_{X'}}^2} \quad (13)$$

Table 3 Experimental uncertainty for all validation cases.

Case	$U_{X'}$	$U_{Y'}$	$U_{N'}$
Hull 1 – Bare	7.6%	8.2%	2.0%
Hull 16 – Bare	9.4%	8.4%	2.4%
Hull 19 – Bare	9.4%	7.6%	2.2%
Hull 34 – Bare	7.6%	8.9%	6.2%
Hull 1 – Rudder	6.8%	6.1%	6.4%
Hull 1 – Bilge Keel	6.3%	5.3%	5.9%
Hull 34 – Skeg	6.6%	5.7%	9.5%
Hull 34 – Skeg+Barkeel	6.1%	5.1%	10%
Max	9.4%	8.9%	10%

5 SIMULATION METHOD

5.1 NUMERICAL MODELLING

Numerical simulations were performed at model scale using the FINE/Marine code, a commercial package developed by Numeca [11]. The flow field around the hulls is calculated using the unsteady Reynolds–Averaged Navier Stokes equations on an unstructured grid. It is understood that flow around the hull operating with a leeway angle is characterized by large anisotropic vortices that constitute the hydrodynamic reaction in the sailing equilibrium [12]. Key modelling issues include the prediction of separation and the location of separation, the trajectory of the shed vortex, and the dissipation of energy within such a structure. The physical motivation for particular attention to the discretization of regions of the domain that contain this pattern of shed vorticity is borne out by a solution verification study [13]. Here it was observed that the thickness of the refinement levels influences the level of data scatter associated with shortcomings in physical modelling. The simulation will be described insofar as is possible within the scope of this paper. The attention will be toward modelling and meshing issues mentioned above.

In light of the large number of hulls to be analysed, turbulence is modelled using the Explicit Algebraic Stress Model (EASM) to provide a balance between the Boussineq-modelling of conventional turbulence models and the more computationally expensive options. It is considered impractical to include large-eddy simulations or other variations of Navier-Stokes simulation in the routine evaluation of hull variants. The evaluation of flow gradients and turbulent stresses is performed with a blended upwind/central scheme based on the local Courant number. The solution for the free surface is determined using the volume of fluid method, involving an interface compression algorithm [11] that is likewise dependent on the local Courant number. For the modelling of sideforce production, numerical dissipation should be minimized, and the third-order central scheme was therefore preferred over the more dissipative upwind scheme. Although the FINE/Marine software is stable for large Courant numbers, the time step was kept relatively small to favour the central scheme in the blended algorithm for flow gradients. A time step equal to $1/500 * (L/U)$ was adopted following a solution verification exercise (upcoming publication).

5.1 MESH CONSTRUCTION

The Drift Sweep procedure [5], was adopted for the analysis of a series of leeway angles and speeds. The domain is meshed once, with the ship aligned with the X-axis, and assigned a prescribed motion within a quiescent fluid. Computing time is presented alongside all results to demonstrate the utility of this approach. The domain is meshed once, with the ship aligned with the X-axis, and assigned a prescribed motion (including a leeway angle) within a quiescent fluid. Simulation cases proceed from a converged solution to the next combination of leeway angle and vessel speed using a gradual transition, such

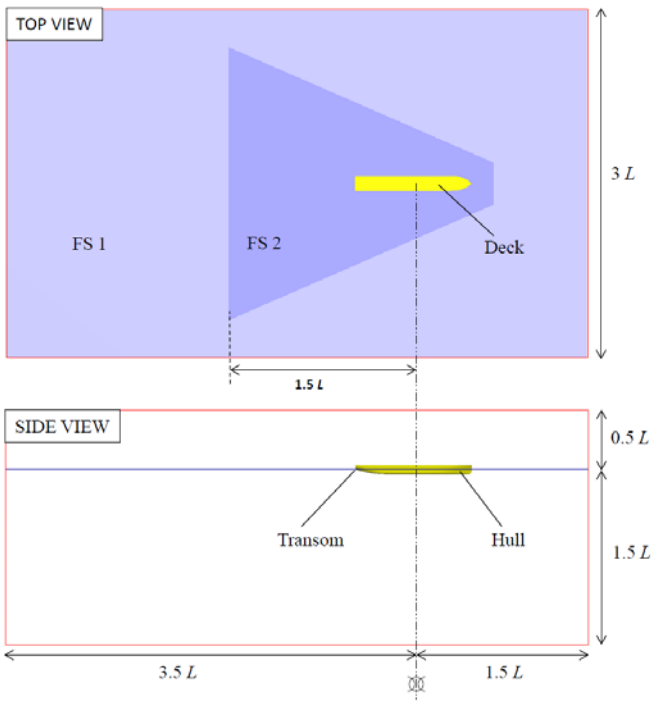

Figure 3 Computational domain for simulation.

that the time required for the convergence of the new solution is reduced compared with reinitializing the computation. Computing time is presented alongside all results to demonstrate the utility of this approach.

The Numeca meshing package, Hexpress, is used to create the mesh. The domain is shown in Figure 3. In the initial meshing step, the domain is uniformly subdivided, with twenty cells along the X-direction. Further subdivisions are made according to the refinement levels set for each surface. There are 500 cells along the length of the hull. The free-surface mesh is defined using two surfaces. The Z-dimension for both surfaces is equal to $L/1000$. The wake of the ship is captured with FS2, where the cell size in X and Y is $L/80$. For the remainder of the free surface, the cell size in X and Y is $L/20$ (these dimensions correspond to the base mesh). Simulations were carried out at model scale, with a relatively low Reynold's number of 2.3E6, and the Y^+ requirements of the log-law wall model were satisfied with four prismatic cells used to resolve the boundary layer. A single mesh is used for a range of vessel speeds, meaning that the Y^+ value varied somewhat. Appendages are meshed using the same cell size as the hull. Additional refinement is added for regions where strong flow gradients are expected: the trailing edge and tip of the rudder, trailing edge and bottom for the skeg and barkeel, and the edges of the bilge keels.

5.2 NUMERICAL UNCERTAINTY

Simulation uncertainty was estimated according to the methodology of Eça and Hoekstra [7, 6] and presented at the 2016 International Conference for Hydrodynamics [13]. Further results, as used for this validation exercise will form the content for a forthcoming journal publication. The simulation verification exercise, which involves simulations for progressively refined grids, is a significant computational effort. Therefore a representative case—Hull 1 - Bare at $Fn = 0.17$ and $\beta = 9^0$—was selected to estimate simulation uncertainty. A direct validation for this case is presented for a fine mesh and a base mesh considered practical for the routine evaluation of hull forms considering the available computational resources.

6 RESULTS

The results for the validation exercise are presented. To begin, a comparison between simulation and experimental resistance values is shown. A good agreement is expected for this routine implementation for RANS-CFD. Next, the direct validation for Hull 1 - Bare at $Fn = 0.17$ and $\beta = 9^{\circ}$ is given, followed by the visualization of the bow wave profile for Hull 34 - Bare. Finally, the validation statement is made for the bare-hull geometries in the Wind Assist series and for select appended geometries.

6.1 RESISTANCE RUNS

Resistance runs for bare hull cases are presented in Figure 4. Results have been non-dimensionalized using the displacement.

$$X'_{\Delta} = \frac{F_X}{\rho g L^3} \tag{14}$$

A resistance curve was measured for Hull 34 – Bare for the estimation of the strip resistance coefficient, and resistance runs are available for Hulls 1, 16, and 19.

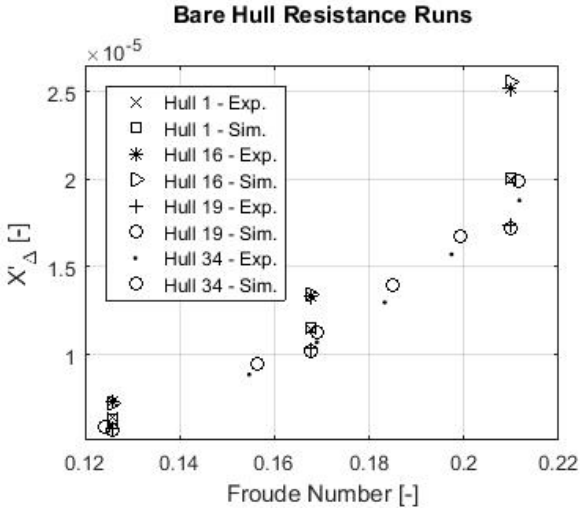

Figure 4 Resistance runs for Bare hull cases, showing experimental and simulation result.

A good agreement is observed for the hulls tested in 2015 whereas an over-prediction of approximately 5 percent is observed for Hull 34 (2016). Recalling the discussion of Sections 2 and 3, hulls tested during the 2015 campaign were free to sink and trim, whereas Hull 34 - Bare was tested in a fully restrained setup in 2016. The simulation for Hull 34 contains fewer modelling errors, since the treatment for trim and sinkage are consistent for the experimental and simulation setup. The over-prediction is attributed to a modelling discrepancy in the treatment of boundary layer between the experiments and simulation. Turbulence stimulators were used to 'trip' the boundary layer in experiments, achieving a fully developed turbulent boundary layer profile along the entire hull. For the model-scale simulation, the boundary layer is allowed to develop as it passes along the ship, apparently giving a larger resistance. Though there is apparently a systematic error present, the magnitude of this error is less than the experimental and simulation uncertainties.

For sailing applications and within the larger framework of this project, the change in resistance due to leeway angle, which includes the induced resistance, is the relevant quantity:

$$X'_i = X' - X'_{\beta=0^{\circ}} \tag{15}$$

This is the change in resistance due to sideforce generation, which will not suffer from a bias as observed in Figure 4.

6.2 EXPLICIT VALIDATION CASE

A direct estimate for all components of the validation standard uncertainty was available for Hull 1 - Bare at $Fn = 0.17$ and $\beta = 9°$. A simulation value and an estimate for the numerical uncertainty on a fine grid was available from the simulation verification exercise. The fine mesh contained 9M cells, requiring 75 hours to perform one simulation with the available computing resources. The base mesh contains 3M cells, and required 11 hours.

Table 4 Validation for Hull 1 – Bare at $Fn = 0.17$ and $\beta = 9^0$.

	$E_{\%}$	U_{Exp}	U_{Num}	u_{Val}
Fine Mesh: 9M Cells, 75 hours				
X_i'	-0.6%	7.6%	5.0%	9.1%
Y'	-6.4%	8.2%	4.9%	9.5%
N'	-0.6%	2.0%	5.2%	5.6%
Base Mesh: 3M Cells, 11 hours				
X_i'	0.0%	7.6%	7.5%	11%
Y'	1.4%	8.2%	15%	17%
N'	1.3%	2.0%	10%	10%

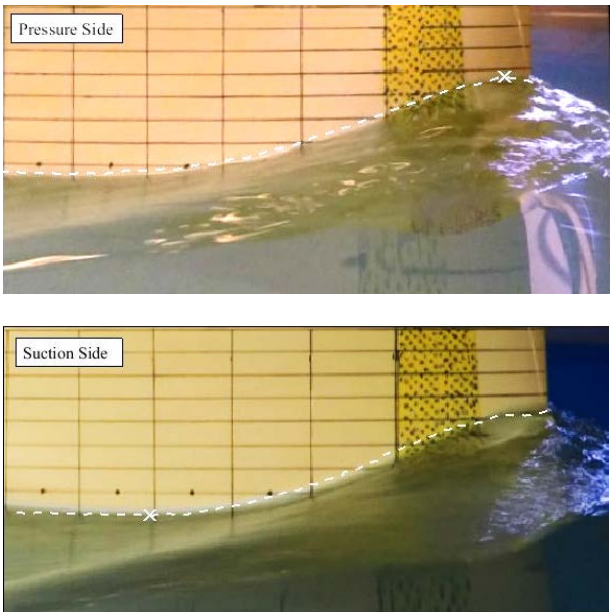

Figure 5 Bow wave profile corresponding to the median error ($Fn = 0.17$ and $\beta = 6^0$). The images have been overlaid with the wave elevation obtained by simulation.

All force components, for both meshes, are validated. It is apparent that the numerical uncertainty is the dominant contribution to the validation standard uncertainty for the base mesh. Details for the comparison error and the validation level are presented in Table 4.

6.3 BOW WAVE PROFILE

The bow wave elevation was measured with cameras and using grid markings on the model. A formal validation statement is not made here, but a good qualitative agreement is observed. A quantitative comparison was made for the maximum bow wave height and location (pressure side), and the minimum wave height and location (suction side). The median error values occurred for $Fn = 0.17$ and $\beta = 6^0$.

6.4 VALIDATION OF RANS-CFD SIMULATION FOR DELFT WIND-ASSIST SERIES

As described in Section 3.3, the 95% confidence interval of the comparison error for the set of validation cases is used to infer a validation statement for the remainder of the wind-assist series. The validation statement is made with results from simulations performed with the base mesh (3M cells). The computation time for one hull for a complete PPP sweep (12 simulations) is six days. This is considered the limit for the batch evaluation of many hull forms.

Table 5 Details of the validation for the Delft Wind-Assist series.

	μ_{Ens}	σ_{Ens}	$CI95_{Ens}$	u_{Val}
Bare Hull Cases: Complete set, N=36				
X_i'	0.0%	4.6%	9.7%	12%
Y'	-2.5%	9.1%	21%	17%
N'	1.1%	5.6%	12%	14%
Bare Hull Cases $\beta = [3^0, 6^0]$, N=24				
X_i'	-0.9%	3.9%	8.9%	12%
Y'	0.0%	6.7%	14%	17%
N'	0.5%	2.9%	6.4%	14%

Results for simulation validation for the complete Wind-Assist series are presented in Table 5. The complete validation set is composed of 36 comparison errors (four hulls, each tested at three speeds and three leeway angles). The mean value, standard deviation, and the 95% confidence interval for the comparison error is given for the complete validation set, and for a set with $\beta = 9^o$ removed. The validation is successful for the abridged set.

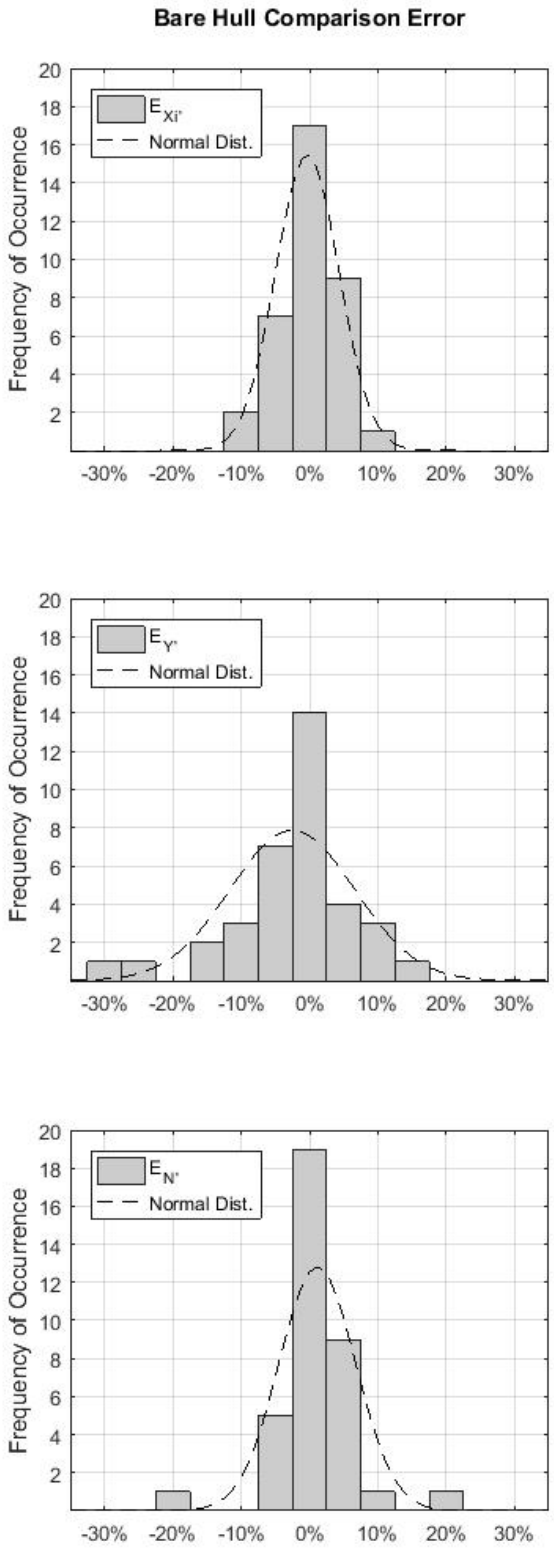

Figure 6 Distribution of comparison error for the complete set of bare hull validation cases (N=36).

The distribution of comparison errors is presented in Figure 7. For the sideforce in particular, the negative outliers correspond to Hull 16 for $\beta = 9^o$. This hull has sharp bilges, where pronounced separation of bilge vortices is expected. Simulation for sideforce is consistently under-predicted for this hull. In contrast, the sideforce for Hull 34 (deadrise hull) is consistently over-predicted. The outliers for the yaw moment correspond to Hull 16 for $\beta = 9^o$.

6.5 VALIDATION FOR APPENDED CASES

Simulation validation for appended cases was successful for select geometries and operating conditions only. The simulation results for the bilge keel case significantly under-predicted the lateral force. The log-law modelling for the boundary layer was not sufficient to capture separation behaviour at the bilge keel. Results for this case are not reported.

Table 6 Details of validation for Hull 1 – Rudder.

	$\mu_{\mathbf{Ens}}$	$\sigma_{\mathbf{Ens}}$	$CI95_{\mathbf{Ens}}$	$u_{\mathbf{Val}}$
Hull 1 – Rudder: Complete Set, N=18				
$\boldsymbol{X_i'}$	2.6%	3.1%	9.1%	12%
$\boldsymbol{Y'}$	-8%	8.1%	25%	17%
$\boldsymbol{N'}$	-1.8%	4.1%	10%	14%
Hull 1 – Rudder: $\beta = [3^0, 6^0]$, N=12				
$\boldsymbol{X_i'}$	1.9%	1.8%	5.9%	12%
$\boldsymbol{Y'}$	-3.4%	1.9%	7.5%	17%
$\boldsymbol{N'}$	-1.7%	2.0%	6.1%	14%

The validation was successful for the Rudder for the validation set with $\beta = 9^o$ omitted. The statistics for the comparison error show better agreement than for bare hull geometries (Table 5). It should be noted that the average comparison error for Hull 1 – Bare was not the lowest of the bare-hull validation cases.

Table 7 Details of validation for Hull 34 – Skeg and Hull 34 – Skeg+Barkeel.

	$\mu_{\mathbf{Ens}}$	$\sigma_{\mathbf{Ens}}$	$CI95_{\mathbf{Ens}}$	$u_{\mathbf{Val}}$
Hull 34 – Skeg: $\beta = [3^0, 6^0]$, N=6				
$\boldsymbol{X_i'}$	2.1%	1.7%	6.3%	12%
$\boldsymbol{Y'}$	3.0%	2.4%	9.0%	17%
$\boldsymbol{N'}$	5.9%	4.8%	18%	14%
Hull 34 – Skeg+Barkeel: $\beta = [3^0, 6^0]$, N=6				
$\boldsymbol{X_i'}$	3.8%	4.3%	14%	12%
$\boldsymbol{Y'}$	4.7%	3.9%	14%	17%
$\boldsymbol{N'}$	8.8%	9.7%	33%	14%

The Skeg and Skeg+Barkeel cases are validated for the sideforce only, when $\beta = 9^o$ is omitted. For these geometries, the simulation over-predicted the yaw

moment in particular, perhaps reflecting an inability to fully capture the separation of flow at the stern.

8 CONCLUSION

The validation exercise for bare-hull cases and appended cases was presented. The validation methodology was described, especially the definition of an ensemble comparison error, E_{Ens}, used for the validation of simulations for the hulls of the Delft Wind-Assist Series. The validation level, u_{Val}, (base mesh, 3M cells) for each force component is: $u_{X'}$=12%, $u_{Y'}$=17%, $u_{N'}$=10%. The experimental method was described, with attention placed on the quantification of uncertainty. The uncertainty for numerical simulation was adopted from an earlier publication devoted to the subject. Aspects of the simulation method that are relevant for modelling the 'sailing condition' for commercial ships were detailed. Finally, a series of validation statements was made for the simulation of hulls from the Delft Wind-Assist Series. First, an explicit validation statement was made for the parent hull of the series, at $Fn = 0.17$ and $\beta = 9°$, for which the validation level for sideforce (fine mesh) was 9.5%. A validation statement for the numerical simulation for hulls from the entire series was made. The statistics of the validation set were used to infer a range of expected values of the comparison error for the complete Wind-Assist Series. The validation statement was made for bare-hull geometries of the Wind-Assist Series with leeway angle $\beta = 9^o$ omitted, giving a validation level for sideforce (base mesh) of 17%. The validation for appended geometries was not regarded as successful, with the exception of the Rudder case. The numerical uncertainty is the dominant contribution for the validation level, motivating a proportionate refinement of the grid. Here, it is sufficient to achieve parity with other contributions to the uncertainty within the larger context of the project.

ACKNOWLEDGEMENTS

This research is conducted with the support of the European Commission as part of the Joules Project. The author would also like to thank the Vaderland Fonds for their support.

REFERENCES

[1] R. T. Jones, "Properties of low-aspect ratio pointed wings at speeds below and above the speed of sound," *NACA report # 835*, 1946.

[2] J. A. Keuning and U. B. Sonnenberg, "Approximation of the hydrodynamic forces on a sailing yacht based on the 'Delft Systematic Yacht Hull Series'," *HISWA Symposium on Yacht Design and Yacht Construction*, pp. 99-152, 1998.

[3] G. Struijk, "Hydrodynamics of Wind Assisted Ship Propulsion," *MSc Thesis*, 2015.

[4] International Towing Tank Commitee, "Uncertainty Analysis in CFD: Verification and Validation, Methodology and Proceedures," 2008.

[5] American Society of Mechanical Engineers, "Standard for Verification and Validation in Computational Fluid Dynamics and Heat Transfer," ASME, 2009.

[6] P. J. Roach, "Quantification of Uncertainty in Computational Fluid Dynamics," *Ann. Rev. of Fluid Mechanics*, vol. 29, pp. 123-160, 1997.

[7] L. Eça and M. Hoekstra, "A Proceedure for the Estimation of the Numerical Uncertainty of CFD Calculations Based on Grid Refinement Studies," *Journal of Computational Physics*, vol. 262, pp. 104-130, 2014.

[8] International Towing Tank Committee, "Recommended Proceedures and Guidelines: Resistance Tests," 2011.

[9] International Towing Tank Commitee, "Force and Moment Uncertainty Analysis for Planar Motion Test," 2008.

[10] Internation Towing Tank Commitee, "Recommended Practices- Uncertainty Analysis in CFD Verification Proceedures," 2008.

[11] Numeca Int, "ISIS Theoretical Manual".

[12] N. J. van der Kolk, "Hydrodynamics of Wind-Assisted Ship Propulsion: Modelling of Hydrodynamic Sideforce," in *HISWA Technical Conference*, Amsterdam, 2016.

[13] N. J. van der Kolk, J. A. Keuning and R. H. M. Huijsmans, "Hydrodynamics of Wind-Assisted Ship Propulsion: Verification of RANS Simulations," in *International Conference for Ship Hydrodynamics*, Egmond aan Zee, 2016.

[14] S. L. Toxopeus, "Practical application of viscous-flow calculations for the simulation of manoeuvering ships," *PhD Thesis*, 2011.

AUTHORS BIOGRAPHY

Ir. N.J. van der Kolk is a Ph.D. researcher in the Ship Hydromechanics Section of Delft University of Technology. He is developing the hydrodynamic models for the TU Delft Wind-Assist Performance Prediction Program.

Dr.ir. J.A. Keuning is an Associate Professor in the Ship Hydromechanics Section of Delft University of Technology.

Prof.dr.ir. R.H.M. Huijsmans is a Professor in the Ship Hydromechanics Section of Delft University of Technology.